Applied Physics B (2019) 125:75
https://doi.org/10.1007/s00340-019-7186-z

Applied Physics B
Lasers and Optics

Selective Hermite–Gaussian mode excitation in a laser cavity by external pump beam shaping

Florian Schepers[1] · Tim Bexter[1] · Tim Hellwig[1] · Carsten Fallnich[1,2]

Received: 13 November 2018 / Accepted: 8 April 2019 / Published online: 15 April 2019

Abstract
An improved gain-shaping method for selective mode excitation is presented and its application for the excitation of higher order Hermite–Gaussian modes is demonstrated in an end-pumped Nd:YVO_4 laser. Using a digital micromirror device, the intensity distribution of the pump beam within the laser crystal could be shaped with a high degree of freedom. Thus, a broad variety of different gain distributions were achieved, enabling a highly selective mode excitation method based on gain shaping. In the presented experiment, the excitation of nearly 1000 different Hermite–Gaussian modes was demonstrated, increasing the number of excitable Hermite–Gaussian modes by at least a factor of five, compared to other excitation methods. The excited modes include Hermite–Gaussian modes of high orders as, for example, the $HG_{25,27}$ mode. Furthermore, the electronic control of the gain profile, applied via the digital micromirror device, enabled automated measurements of the selective mode excitation. Here, a systematic study is presented to optimize the generated pump patterns with respect to the number of modes that could be excited.

1 Introduction

The transverse eigenstates of free-space lasers are best approximated by either Hermite–Gaussian (HG), Laguerre–Gaussian (LG), or Ince–Gaussian (IG) modes, where the latter constitute the continuous transition between HG and LG modes [1, 2]. Due to their unique phase and amplitude structure, these transverse modes are of great interest for various fields of application, e.g., for laser tweezers [3–6], nano-scale structure fabrication [7], or stimulated emission depletion (STED) microscopy [8]. An extra-cavity generation of these modes can be achieved by shaping the amplitude and phase of an incident beam using a spatial light modulator (SLM) [9] or a digital micromirror device (DMD) [10, 11]. These approaches can already achieve a high mode purity which in some cases can be further improved using a subsequent passive cavity as a premode cleaner [12]. However, modes directly excited in an active laser, from now on referred to as intra-cavity excited modes, significantly differ from the extra-cavity generated modes, as they exhibit a mode-order-dependent frequency shift [1]. The superposition of these modes is, therefore, time dependent and enables spatio-temporal applications as, for example, transverse mode locking [13]. Thus, the direct excitation of modes in free-space lasers is of great interest and different excitation methods have been investigated [14–22]. Even though the excitation of LG modes in a free-space laser can be achieved [14, 15], most lasers favor the operation in an HG basis set, due to a rectangular symmetry resulting from tilted surfaces or distorted elements [1]. However, using a mode converter based on a cylindrical lens pair, as presented by Beijersbergen et al. [23], single HG modes of arbitrary mode numbers m and n can be converted into LG modes with the corresponding mode numbers $p = \min(m, n)$ and $l = m - n$.

A high selectivity for HG mode excitation was achieved by approaches that apply additional intra-cavity components, to modulate the amplitude or phase of the laser light within the cavity [21, 22]. Here, especially, the 'digital laser', in which one of the cavity mirrors is replaced by an SLM, has proven to enable the excitation of a variety of different electric field distributions in the laser cavity including the HG mode set [22, 24]. However, due to the intra-cavity SLM, a drastic increase of the cavity loss of up to 20% was reported for the digital laser, while the intra-cavity intensity

✉ Florian Schepers
f.schepers@uni-muenster.de

[1] Institute of Applied Physics, Westfälische Wilhelms-Universität, Corrensstraße 2, 48149 Münster, Germany

[2] Laser Physics and Nonlinear Optics Group, MESA+ Institute for Nanotechnology, University of Twente, 7500 AE Enschede, The Netherlands

was limited by the low damage threshold of the SLM. To avoid such additional intra-cavity components, gain-shaping-based methods can be used [16–20]. As in these methods, the selective HG mode excitation was achieved via an extra-cavity alteration of the pump light, no modifications of the cavity itself were required. However, so far, all of these approaches were strongly limited with respect to the number of HG modes that could be excited. For example, the approach presented by Sato et al. [20], which was based on the selective mode excitation by unicursal fast scanning of the pump beam, enabled an adjustment-free and fast mode switching between HG, LG, and IG modes. Nevertheless, the excitable modes were limited to relatively low mode numbers, e.g., for the HG modes, only the excitation of either $HG_{0,n}$ or $HG_{m,0}$ modes with $m, n \leq 2$ could be demonstrated. Furthermore, the time-varying position of the pump spot caused strong temporal fluctuations of the output beam.

Here, we demonstrate in a free-space laser an improved gain-shaping method that enables the selective excitation of nearly 1000 different higher order $HG_{m,n}$ modes with arbitrary mode numbers m and n each up to a value 34. Using a DMD, the intensity distribution of the pump beam was modulated in such a way that it matched a binary representation of the transverse intensity profile of a specific targeted mode when imaged onto the laser gain medium. As a result, the intra-cavity gain was optimized for this specific mode, such that the laser oscillated in the targeted mode. Similar to other gain-shaping methods [16–20], no additional intra-cavity components were required, which makes the presented method well suited for the excitation of higher order modes (HOMs) in lasers with, e.g., low cavity losses or limited intra-cavity space [25]. If the micromirrors of the DMD were held in a static position, the continuous pumping of the gain medium by the spatially shaped pump beam enabled a continuous-wave (cw) operation of the laser. The pump pattern displayed by the DMD was fully computer-controlled and could thus be switched automatically. Exploiting this automation capability of the presented gain-shaping method, a systematic measurement was performed, identifying the optimal pattern threshold for the binary pump pattern generation with respect to the number of modes that could be excited.

2 Method and experimental setup

The setup for the DMD-controlled, high-order mode excitation is schematically displayed in Fig. 1a. A DMD (Texas Instruments: DLP4500NIR) was used to spatially shape the intensity profile of the pump light at a wavelength of 808 nm, that was emitted by a fiber-coupled laser diode (LD; BWT: K808DA5RN-35.00W). The DMD consisted of an array of 912 × 1140 micromirrors, which were organized

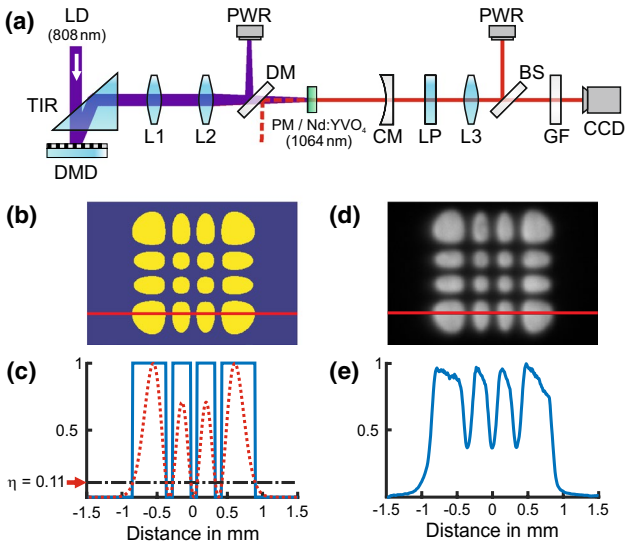

Fig. 1 **a** Schematic of the gain-controlled higher order mode laser setup. For abbreviations, see the setup description in the text. **b** Binary pump pattern calculated for the $HG_{3,3}$ mode with a pattern threshold of $\eta = 0.11$ and **d** corresponding CCD image of the fluorescence emitted by the pumped laser crystal. The horizontal red lines in (**b**, **d**) mark the positions of the cross sections displayed with solid blue lines in (**c**, **e**), respectively. In addition, the cross section of the normalized intensity distribution of the $HG_{3,3}$ mode (dashed red line) and the pattern threshold $\eta = 0.11$ (dashed–dotted black line) are displayed in (**c**)

in a diamond configuration. The individual micromirrors had a size of 7.6 µm × 7.6 µm and could be tilted along their diagonal axis either into an 'on-' or 'off-state'. The light reflected by the micromirrors in the 'off-state' was discarded and directed into a beam dump. The light reflected by the micromirrors in the 'on-state', however, was separated from the incident light by a total internal reflection prism (TIR) and imaged onto the laser crystal via two lenses (L_1, L_2) with focal lengths $f_1 = 125$ mm and $f_2 = 100$ mm, respectively. Therefore, the transverse intensity distribution of the pump beam within the crystal, and thus, the spatial gain distribution of the laser could be controlled by the DMD. Due to the periodically structured micromirror array, the light reflected from the DMD was diffracted into multiple diffraction orders [26]. To reduce the diffraction losses, the imaging lenses were aligned, such that the four diffracted beams with the highest pump power, from now on referred to as pump beams, were superposed with each other in the image plane at the laser crystal. This results in a total transmission of about 35% for the combined optical system of TIR, DMD, telescope, and DM if all micromirrors were in the 'on-state'.

The imaging ratio of the pump pattern from the DMD to the laser crystal was 0.73 and a minimum resolvable pump spot size within the image plane of 35 µm × 35 µm could experimentally be measured. Beyond the image plane, the

effective resolution was reduced as the four pump beams diverged in the transverse direction by 90 µm per millimeter along the optical axis. Thus, the effective transverse gain profile generated by the pump light in an active gain medium would become blurred with increasing length of the gain medium. As a result, the overlap of the effective gain profile with competing modes would increase, and accordingly, the selectivity of the excitation method would decrease. Therefore, a short active gain medium was important to achieve a high modal selectivity, while simultaneously, the gain medium had to be long enough to provide sufficient gain for laser oscillation also of high-order modes. In our experiments, a crystal length of 1mm has proven to be appropriate to achieve laser operation as well as a selective excitation of the targeted modes. Simultaneously, the clear aperture of the crystal in the transverse direction was chosen to be relatively wide (6mm × 6mm) compared to the crystal length to accomplish the oscillation of modes of high mode numbers without significant diffraction losses.

For the selective mode excitation we chose an end-pumped Nd:YVO_4 laser with a plano-concave two-mirror cavity geometry. The YVO_4 crystal was a-cut and had an 1 at.% Nd-doping concentration. Due to a highly reflective coating for the laser light at 1064nm wavelength the outward facing side of the crystal served as the plane mirror (PM) of the laser cavity. The intra-cavity side of the crystal was coated with a highly transmissive coating for the laser wavelength, while both sides of the crystal were anti-reflective coated for the pump wavelength at 808nm. The laser cavity was closed by a curved ($R = 1$m) and highly reflective ($r = 99.992\%$ at 1064nm) dielectric mirror (CM), resulting in a cavity length of 345mm. The fundamental mode beam waist in the laser crystal was calculated to be $w_0 = 401$ µm, which was in good agreement with the measured beam waist of $w_{exp} = 394 \pm 10$ µm.

The high reflectivity of both cavity mirrors ($r > 99.8\%$) resulted in low lasing thresholds (e.g., 27mW of pump power for the $HG_{0,0}$) for the HOMs and were chosen to achieve laser oscillation at low pump powers. Furthermore, it demonstrates that our approach is well suited for the application in laser cavities which require low cavity losses. Laser light was coupled out via both cavity mirrors, as the PM as well as the CM had a remaining transmission at the laser wavelength of 0.11% and 0.008%, respectively. The laser light coupled out via the PM was separated from the incident pump light by a dichroic mirror (DM) with a highly transmissive coating at the pump wavelength of 808nm and a highly reflective coating at the laser wavelength of 1064nm. As a reference for the pump power incident on the laser crystal, the residual pump light reflected by the DM could be measured with a power meter (PWR). We chose the CM as output for our measurements, as the best imaging of the laser modes was achieved from this side. Using a long-pass filter (LP) with a cut-off wavelength of 1050nm, the pump light was removed from the out-coupled laser light. While the majority of the remaining laser light was directed via a lens L_3 ($f_3 = 200$ mm) and a beam splitter (BS) onto a power meter, a minor part of the laser light was transmitted through the BS and detected with a CCD-camera, which was protected against saturation with a gray filter (GF). Using L_3, the plane of the laser crystal was imaged onto the CCD-camera.

When selectively exciting HOMs by gain shaping, it is not only important to ensure that the created gain profile has a sufficient overlap with the targeted mode, but also that the overlap of the gain profile with other modes of the cavity is minimized. Otherwise, simultaneous laser oscillation of competing transverse modes can occur and even suppress laser oscillation of the targeted mode. The most straightforward approach to achieve such selective gain shaping would be to match the intensity distribution of the pump light to the intensity distribution of the targeted mode. However, as the DMD by design only supports binary patterns, the representation of continuous intensity distributions could only be approximated by a superpixel segmentation of the DMD [11], which would result in intolerably high losses of the pump power. Consequently, it was more suitable to identify binary pump patterns, which provided a sufficient differentiation between the individual modes. Taking into account that Hall et al. [27] have shown that for the efficient excitation of a fundamental Gaussian beam, the size of the pump spot is more important than the exact shape of the pump distribution, we defined the binary pattern for a certain HG mode in the following way: for all points of its normalized intensity distribution above a given pattern threshold $0 \leq \eta \leq 1$, the pump light pattern was set to one (micromirror in 'on-state'), and for all points below η, the pattern was set to zero (micromirror in 'off-state'). Thus, in the case of an arbitrary mode, the binary pump pattern consisted of multiple spots which resembled the intensity maxima of the targeted mode in position, size, and geometry. The size of these spots and, therefore, the effective area of the pattern increased with decreasing η and vice versa. The identification of the optimal pattern threshold η with respect to the number of excitable modes will be part of the subsequent investigations.

An example for a binary pump pattern, calculated at a pattern threshold of $\eta = 0.11$ for the $HG_{3,3}$ mode, can be seen in a false color representation in Fig. 1b. In the cross section of the binary pattern displayed in Fig. 1c, it can be seen that the pattern is zero for all values of the normalized intensity distribution (dashed line) below the pattern threshold η (dashed–dotted line) and one for all values above η. As an indicator for the resulting effective transverse gain distribution of the laser, the fluorescence of the excited laser crystal was measured, which is depicted in Fig. 1d. A comparison of the fluorescence with the binary pump pattern (see Fig. 1b) demonstrates the

successful shaping of the gain profile via the DMD. Nevertheless, within the cross section of the fluorescence displayed in Fig. 1e, deviations from the cross section of the applied binary pump pattern (see Fig. 1b) could be observed. These deviations were caused by aberrations of the imaging optics and by imperfections in the laser gain medium, which for instance resulted in a non-zero fluorescence at the local minima of the generated gain distribution (see Fig. 1e). However, as will be seen in the following, these deviations from the binary pump pattern were sufficiently small to allow a clear discrimination between the different excited $HG_{m,n}$ modes.

3 Results and discussion

Using the described method of gain shaping, a selective excitation of arbitrary $HG_{m,n}$ modes was possible. For a selected number of these modes, the fluorescence images indicating the generated gain distribution and the resulting laser intensity distribution can be seen in Fig. 2a–d and e–h, respectively. All depicted modes were excited by pump patterns with a pattern threshold of $\eta = 0.11$. The dimensions of the laser crystal can be seen in the fluorescence images due to the fluorescent light scattered from the crystal's edges. In both dimensions, modes with mode numbers of up to at least 34 (Fig. 2f, g) could be excited and also the excitation of two-dimensional modes of high mode numbers such as the $HG_{25,27}$ mode (Fig. 2h) could be measured. The $HG_{25,27}$ consists of 728 individual intensity peaks which are aligned in a rectangular array. Such a high variety of HG modes excited in a laser cavity has so far not been achieved by any other spatial gain shaping method [16–20]. The achieved mode numbers are significantly extended, compared to the typically reported highest mode numbers such as the $HG_{7,7}$ or $HG_{22,0}$ mode [19, 21]. Higher mode numbers up to the $HG_{90,0}$ or $HG_{0,90}$ modes were only presented by Laaps et al. [16], whose method was limited to the excitation of solely $HG_{m,0}$ or $HG_{0,n}$ modes.

The initial pump power in front of the pump beam-shaping setup was 6.8W of which an effective pump power of 2.4W reached the laser crystal if all micromirrors were in the 'on-state'. However, as the transmitted pump power of the system was reduced proportionally with the number of illuminated micromirrors in the 'off-state', the effective pump power incident on the laser crystal was dependent on the applied binary pump pattern. Therefore, HOMs received a higher effective pump power P_{Pump} with increasing mode numbers m and n.

The laser threshold of the fundamental and HOMs is proportional to the effective mode volume [28]:

$$V_{\mathrm{eff}} = \left(\iiint_{\mathrm{crystal}} s_{m,n}(x,y,z) r_{m,n}(x,y,z)\, \mathrm{d}V \right)^{-1}, \quad (1)$$

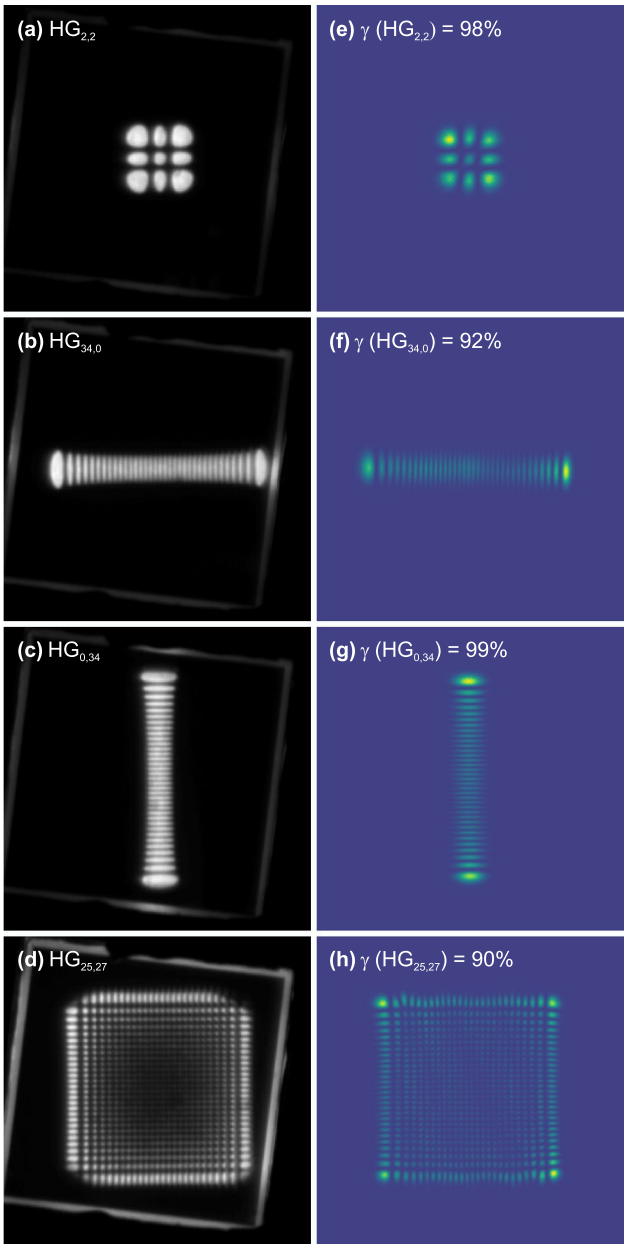

Fig. 2 Measured profiles of the fluorescence (**a–d**) and the resulting laser intensity distribution (**e–h**) of the $HG_{2,2}$, $HG_{34,0}$, $HG_{0,34}$, and $HG_{25,27}$ mode. The binary pump patterns used for the mode excitation were calculated with a pattern threshold of $\eta = 0.11$. For each of the measured laser intensity distributions, the corresponding correlation coefficient γ is given

of the normalized photon density distribution of the laser mode $s_{m,n}$ and the applied normalized pump rate distribution $r_{m,n}$ within the laser crystal volume. When applying Eq. 1 to the binary pump patterns used in the here presented experiment, an increasing V_{eff} with increasing mode numbers m and n, and thus, a rising laser threshold is predicted. This trend is in excellent agreement with our experimental results for low mode orders ($m, n < 10$). For higher mode

orders, the laser threshold increases slightly stronger then predicted by the theoretical model and a deviation of up to a factor of 1.45 has been measured. The most probable explanation for the increased laser threshold at higher mode orders are mode-dependent round-trip losses due to cut-off effects or imperfections of the intra-cavity optics, which are not accounted for by the above calculated effective mode volume.

As the laser threshold and effective pump power did not scale equally with the mode numbers m and n, they did not compensate each other and, hence, a varying output power for different HOMs could be observed. For instance, at $\eta = 0.11$, the total laser output power increased from a value of 12.68mW (0.86mW via CM and 11.81mW via PM) for the $HG_{0,0}$ mode ($P_{\mathrm{Pump}} = 70$mW) up to a maximum value of 39.33mW (2.68mW via CM and 36.66mW via PM) for the $HG_{5,12}$ mode ($P_{\mathrm{Pump}} = 304$mW) and decreased again for modes of higher mode numbers. As the presented work focused on the excitation of a high number of different HG modes, rather then on high output powers, the achieved power values are relatively low, but still comparable to the output power of about 12mW for the fundamental mode achieved by Ngcobo et al. with an intra-cavity SLM [22]. In contrast to an efficiency of about 0.06% [22], we achieved with our DMD-based setup, a three time higher overall efficiency for the fundamental mode of 0.19%, considering the pump beam shaping and the laser efficiency. Higher outcoupling ratios could increase the output efficiency for the lower order HG modes, but would also reduce the number of modes that can be excited. Nevertheless, the current development of further improved DMDs for the near-infrared wavelength region might enable significantly increased pump powers of multiple tens of Watts. Such high pump powers would not only increase the output power itself, but would also shift the optimal outcoupling ratio for all modes to higher values and thus enable more efficient coupling ratios [1]. However, with increased pump powers, also thermal lensing effects would have to be considered. So far, these effects could be neglected as the effective pump power at the laser crystal was sufficiently low to have no measurable impact on the beam quality. This was verified by a theoretical analysis based on the analytic approximation presented by Innocenzi et al. [29] and an experimental beam characterization measurement. For pump powers beyond a few 100 mW, however, the refractive power of the thermal lens would obtain a considerable influence on the laser geometry and result in changes of the cavity eigenmodes. As for high pump powers, this can result in pump pattern dependent thermal lens structures, different approaches can be applied to reduce thermal lensing effects. For example, composite laser crystals can be used to extract heat from the active gain medium through the undoped end faces [30], or if Nd:YAG is used as a gain medium, cryogenic cooling can strongly increase the thermal conductivity and thus flatten the temperature profile within the laser crystal [31, 32]. In addition, the high degree of freedom given by the DMD provides a straight forward possibility to actively adjust the pump pattern to compensate potential perturbations induced by thermal lensing effects.

If the micromirrors of the DMD were held in a fixed position, the intensity fluctuations of the excited laser modes were typically about 3%, calculated from the standard deviation of a photodiode trace that was measured over a time period of 1 min. Thus, due to the constant pump pattern, the temporal fluctuations were reduced by a factor of 15 compared to the fluctuations of about 46%, which have been observed for the mode excitation method by a fast unicursal scanning pump beam (data extracted from Fig. 6(b) in [20]).

When switching the pump pattern from one mode to another, a corresponding change of the laser intensity distribution within a minimum resolvable time span of 50 µs could be measured with a triggered CCD-camera. Nevertheless, as to be expected for solid-state lasers [1], each mode required a certain settling time before it reached a stable cw operation. In the optimal case, the settling time was limited only by the damping time of the relaxation oscillations of the laser [33], which was in the order of 50 µs. However, for most modes, in addition to the relaxation oscillations, strong fluctuations at a high frequency were measured by the PD, which in average required a settling time of 40 ± 20ms. For the selected number of modes that were investigated, a trend of increasing settling times with increasing mode numbers m and n could be measured. No dependence of the settling time on the previous displayed pump pattern was observed. A radio-frequency analysis has shown that the dominant frequency of these fluctuations matched the frequency of the longitudinal mode spacing. Therefore, a longitudinal mode competition [34] is the most probable cause of these fluctuations, limiting the mode switching frequency in this setup to a few Hz. Whether the operation characteristics of the DMD itself contributed to the extended time scale of the longitudinal mode settling time would require further investigations. Much higher switching frequencies should be possible if the longitudinal mode competition would be suppressed, e.g., by reducing the cavity length or by inserting an etalon into the cavity. Then, the next limiting factor would be the DMD, which supports switching frequencies of about 4.255kHz with a micromirror switching time of 16 µs and an additional minimum dead time of 219 µs.

The orientation of the HG modes was affected by the transverse position of the optical cavity axis on the laser crystal and could vary between the individual modes. Possible explanations for this change in the mode orientation could be a slight bend of the laser crystal, due to its fixation in the crystal holder, as well as impurities in or on the laser crystal. The influence of an intra-cavity loss structure on the

modal orientation has already been previously observed by Chu et al. [21]. Our hypothesis seems to be justified as by carefully realigning the laser cavity a fixed mode rotation of 6.7° relative to the crystal axis could be achieved with a standard deviation of 1.4° between the modes.

In the following, the influence of the pattern threshold η on the number of excitable modes was investigated. For this purpose, the binary pump patterns of all $HG_{m,n}$ modes with $m, n \leq 40$ were calculated for different values of η and displayed on the DMD. For each pump pattern, the resulting intensity distribution of the laser was detected on the CCD-camera and compared to the targeted mode. As a measure, whether a certain mode was successfully excited or not, the correlation of the measured intensity distribution with the numerically calculated intensity distribution of the targeted mode was used. For these correlation calculations, small deviations in the modal position, size, and orientation were considered to find the highest possible normalized correlation coefficient γ. A mode was considered as successfully excited if $\gamma \geq 0.9$, which was verified as a reasonable choice during our experiments as well as in previous studies [9]. Examples of different successfully excited $HG_{m,n}$ modes and their corresponding normalized correlation coefficient γ can be found in Fig. 2.

In Fig. 3, the number of modes that could be excited with $\gamma \geq 0.9$ for different values of η are depicted. As with increasing η, an increasing number of the micromirrors were switched into the 'off-state', the effective pump power was strongly reduced and no laser oscillation could be observed for $\eta \geq 0.75$. With decreasing η, the effective pump power increased resulting in an increasing number of successfully excited HOMs. Simultaneously, the spatial expansion of the pumped gain area reduced the differentiability between the individual modes, such that for low values of $\eta \leq 0.045$, a selective excitation of HOMs became nearly impossible. Instead, either superpositions of multiple modes or modes of deviating mode number were excited. In between these two extrema, an optimal balance of available pump power and modal differentiability was observed at a pattern threshold of $\eta = 0.11$, for which the highest number of 966 individual modes could be selectively excited. Compared to previously presented HG mode excitation methods, this corresponds to an increase of excitable modes by at least a factor of five [16–22]. At the optimal pattern threshold of $\eta = 0.11$, the binary pump spot for the fundamental mode had a radius of $415 \pm 10\,\mu m$ on the laser crystal, which is only slightly above the measured $1/e^2$-width of the fundamental mode of $w_{exp} = 394 \pm 10\,\mu m$.

The normalized correlation coefficients γ of the different modal intensity profiles measured for a pattern threshold of $\eta = 0.11$ are depicted in a false color representation in Fig. 4. It can be seen that the successfully excited modes form a continuous area reaching from the fundamental mode up to the $HG_{34,0}$ mode or $HG_{0,36}$ mode in the x- and y-directions, respectively, and up to the $HG_{25,27}$ mode in the diagonal direction. In average, the correlation coefficient γ of the successfully excited modes was 0.96 ± 0.02, which is comparable to the correlation values reaching from about 0.89–0.99 achieved for 13 different low-order LG modes by extra-cavity mode generation based on an SLM [9].

As can be seen from the fluorescence images in Fig. 2b–d, for modes with a very high mode number, the intensity distribution reached the edges of the laser crystal, such that the HOMs experienced a cutoff with increasing mode number related to increased diffraction losses. In Fig. 4, this becomes apparent by a drop of the normalized correlation coefficients γ below 0.9. For an orthogonal orientation of the modes with respect to the crystal axis it would be expected that the cutoff for the $HG_{m,n}$ modes occurs at a constant mode number m and n in x- and y-directions, respectively. However, as the modes were slightly tilted by an angle of $6.7° \pm 1.4°$, it could

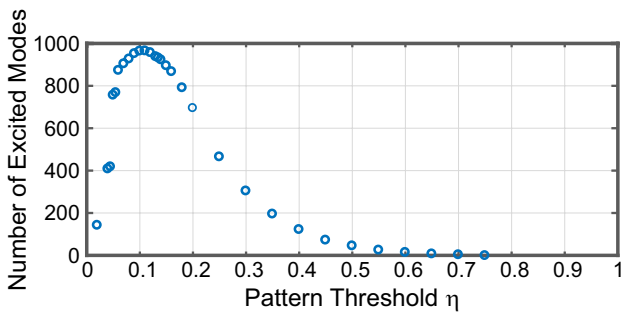

Fig. 3 Number of successfully excited HG modes, i.e., $\gamma \geq 0.9$ for different pattern thresholds η. The maximum of 966 selectively excited modes have been observed for $\eta = 0.11$

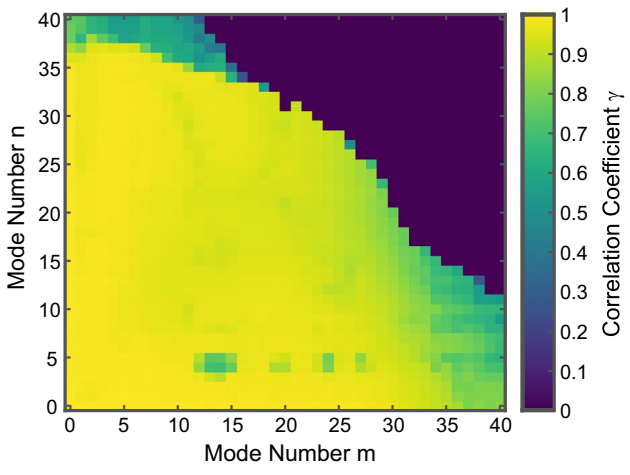

Fig. 4 Normalized correlation coefficients γ of the measured modes with the targeted modes for different mode numbers m and n at $\eta = 0.11$ depicted in a false color representation

be observed that the cutoff occurred at modes with a decreasing mode number m or n if the mode number in the orthogonal direction (i.e., n or m, respectively) was increased. For two-dimensional modes with very high mode numbers m and n, an additional limitation, due to the circular shape of the illuminated area on the DMD, has to be considered. In Fig. 2d, this becomes apparent, as the gain distribution of the $HG_{25,27}$ mode was cutoff at the corner spots, which are outside of the circularly shaped pump beam distribution incident on the DMD. Thus, for even higher mode numbers, an increasing part of the modal distribution will not be pumped and the pump efficiency will be reduced. The separate excitation of adjacent HG modes with high mode numbers demonstrated that a high degree of modal selectivity can be achieved via the presented gain-shaping technique. Excitation of even higher mode orders ($m > 34, n > 36$) might be possible if the gain-shaping method would be applied in a cavity geometry with a smaller beam waist w_0 or in a laser cavity with an extended size of the laser crystal. However, when considering the excitation of even higher mode orders, it is important to keep in mind that the feature sizes of the modes become smaller with increasing mode orders. For example, the smallest feature of the binary pump pattern used for the excitation of the $HG_{25,27}$, as displayed in Fig. 2h, was about $30\,\mu m \times 30\,\mu m$, which is already slightly smaller then the minimum resolvable spot size of $35\,\mu m \times 35\,\mu m$ of our setup. In how far an insufficient resolution would affect the selective excitation of modes of even higher order would require further investigations.

Four areas in the vicinity of the $HG_{14,4}$, $HG_{20,4}$, $HG_{24,5}$, and $HG_{25,27}$ modes can be identified in Fig. 4, where the normalized correlation coefficients γ are reduced below 0.9, indicating that no pure mode excitation had been achieved. As for slight changes in the crystal position, the disturbances were moved to $HG_{m,n}$ modes with adjacent mode numbers, the most likely explanation for these aberrations are small, localized impurities on or in the laser crystal, whose existence could be verified under a bright-field microscope. However, by increasing the pattern threshold η to values above 0.18, which resulted in a more distinct pump pattern, a pure excitation of these modes became possible again. Hence, minor crystal impurities could be compensated by an adjustment of the pattern threshold η or by small readjustments of the laser cavity.

4 Conclusion

In conclusion, due to the application of an improved gain-shaping method for selective mode excitation, the excitation of 966 different HG modes has been demonstrated in an Nd:YVO_4 laser. The number of excitable HG modes was, therefore, increased by at least a factor of five compared to other excitation methods [16–22]. Using a DMD to shape the intensity distribution of the pump beam, a broad variety of different gain distributions could be realized. Thus, a high degree of freedom for the selective mode excitation was achieved, as could be demonstrated by the excitation of all modes up to the $HG_{34,0}$, $HG_{0,36}$, and $HG_{25,27}$ mode. The excitation of even higher mode orders was mainly limited by the finite size of the laser crystal. The application of the DMD enabled a temporally stable mode excitation, while an adjustment-free and computer-controlled switching of the modes was achieved in this particular setup with switching times of about 40 ± 20ms. The high automation capability of the presented method was demonstrated in a systematic measurement, by identifying the optimal pattern threshold of $\eta = 0.11$ with respect to the number of modes that could be excited. Furthermore, the systematic investigations showed that at the cost of the total effective pump power, minor crystal impurities could be compensated by choosing a higher pattern threshold η, i.e., by applying a more distinct pump pattern. In general, no fundamental limitations could be observed that would prevent the excitation of LG or IG modes with this excitation method if a cylindrical symmetry for LG modes or an elliptical symmetry for IG modes would be introduced into the laser cavity. Besides the excitation of single HOM, the investigated gain-shaping method has further potential for the controlled excitation of linear combinations of multiple cavity modes, which allow, for instance, the selective generation of vortex array beams straight from the laser cavity [35] or could be of great value for the generation of a Poissonian-distributed mode content for transverse mode-locked lasers [13].

References

1. A.E. Siegmann, *Lasers* (University Science Books, Mill Valley, 1986), p. 574. (648, 479, 954–969)
2. M.A. Bandres, J.C. Gutiérrez-Vega, Opt. Lett. **29**, 144–146 (2004)
3. S. Sato, M. Ishigure, H. Inaba, Electron. Lett. **27**, 1831–1832 (1991)
4. M. Woerdemann, C. Alpmann, C. Denz, Appl. Phys. Lett. **98**, 111101 (2011)
5. K.T. Gahagan, G.A. Swartzlander, Opt. Lett. **21**, 827–829 (1996)
6. S.H. Tao, X.-C. Yuan, J. Lin, X. Peng, H.B. Niu, Opt. Express **13**, 7726–7731 (2005)
7. K. Toyoda, K. Miyamoto, N. Aoki, R. Morita, T. Omatsu, Nano Lett. **12**, 3645–3649 (2012)
8. S.W. Hell, J. Wichmann, Opt. Lett. **19**, 780–782 (1994)
9. N. Matsumoto, T. Ando, T. Inoue, Y. Ohtake, N. Fukuchi, T. Hara, J. Opt. Soc. Am. A **25**, 1642–1651 (2008)
10. S.A. Goorden, J. Bertolotti, A.P. Mosk, Opt. Express **22**, 17999–18009 (2014)
11. Y.-X. Ren, Z.-X. Fang, L. Gong, K. Huang, Y. Chen, R.-D. Lu, J. Opt. **17**, 125604 (2015)
12. P. Fulda, K. Kokeyama, S. Chelkowski, A. Freise, Phys. Rev. D **82**, 012002 (2010)
13. D. Auston, IEEE J. Quantum Electron. **4**, 420–422 (1968)

14. J.W. Kim, J.I. Mackenzie, J.R. Hayes, W.A. Clarkson, Opt. Express **19**, 14526–14531 (2011)
15. Y. Chen, Y. Lan, S. Wang, Appl. Phys. B **72**, 167–170 (2001)
16. H. Laabs, B. Ozygus, Opt. Laser Technol. **28**, 213–214 (1996)
17. Y.F. Chen, T.M. Huang, C.F. Kao, C.L. Wang, S.C. Wang, IEEE J. Quantum Electron. **33**, 1025–1031 (1997)
18. K. Shimohira, Y. Kozawa, S. Sato, Opt. Lett. **36**, 4137–4139 (2011)
19. W. Kong, A. Sugita, T. Taira, Opt. Lett. **37**, 2661–2663 (2012)
20. T. Sato, Y. Kozawa, S. Sato, Opt. Lett. **40**, 3245–3248 (2015)
21. S.-C. Chu, Y.-T. Chen, K.-F. Tsai, K. Otsuka, Opt. Express **20**, 7128–7141 (2012)
22. S. Ngcobo, I. Litvin, L. Burger, A. Forbes, Nat. Commun. **4**, 2289 (2013)
23. M.W. Beijersbergen, L. Allen, H.E.L.O. van der Veen, J.P. Woerdman, Opt. Commun. **96**, 123–132 (1993)
24. K.-F. Tsai, S.-C. Chu, Laser Phys. **28**, 075801 (2018)
25. J. Klaers, J. Schmitt, F. Vewinger, M. Weitz, Nature **468**, 545–548 (2010)
26. Y.-X. Ren, R.-D. Lu, L. Gong, Ann. Phys. **527**, 447–470 (2015)
27. D.G. Hall, R.J. Smith, R.R. Rice, Appl. Opt. **19**, 3041–3043 (1980)
28. K. Kubodera, K. Otsuka, J. Appl. Phys. **50**, 653–659 (1979)
29. M.E. Innocenzi, H.T. Yura, C.L. Fincher, R.A. Fields, Appl. Phys. Lett. **56**, 1831–1833 (1990)
30. Y.T. Chang, Y.P. Huang, K.W. Su, Y.F. Chen, Opt. Express **16**, 21155–21160 (2008)
31. L. Cini, J. I. Mackenzie, Appl. Phys. B **123**, 273 (2017)
32. H. Glur, R. Lavi, T. Graf, IEEE J. Quantum Electron. **40**, 499–504 (2004)
33. W. Koechner, *Solid-state laser engineering*, 6th edn. (Springer Science+Business Media Inc., New York, 2006), pp. 128–132
34. L.M. Narducci, J.R. Tredicce, L.A. Lugiato, N.B. Abraham, D.K. Bandy, Phys. Rev. A **33**, 1842–1854 (1986)
35. K. Otsuka, S.-C. Chu, Opt. Lett. **34**, 10–12 (2009)